Evaluation of Different Implementations of the Thomson Liquid Drop Model: Comparison to Monovalent and Divalent Cluster Ion Experimental Data

William A. Donald and Evan R. Williams*

Department of Chemistry, University of California, Berkeley, California 94720-1460

Received: November 19, 2007; In Final Form: January 25, 2008

The Thomson model, used for calculating thermodynamic properties of cluster ions from macroscopic properties, and variations of this model were compared to each other and to experimental data for both hydrated mono- and divalent ions. Previous models that used the Thomson equation to calculate sequential binding thermodynamic values of hydrated ions, either continuously or discretely including an ion-dipole interaction term, were compared to a discrete model that includes the excluded volume of an impurity ion. All models, given their limitations, provided reasonable agreement to data for monovalent ions. For divalent cluster ions, the continuous model, and a discrete model that includes the ion-exclusion volume provide significantly better agreement to both the binding enthalpy and the binding entropy data as compared to the model that includes an ion-dipole term. A systematic deviation in the continuous model resulted in significantly lower binding enthalpies than the discrete model for clusters with fewer than about nine and 19 water molecules for mono- and divalent ions, respectively, but this difference became negligible for larger clusters. Previous investigations of the various Thomson model implementations used parameters for bulk water at 313 K. Using parameters at 298 K has a negligible effect at small cluster sizes, but at larger sizes, the binding enthalpies are 0.2 kcal/mol higher than with the 313 K parameters. Although small, the effect is significant for ion nanocalorimetry experiments in which thermochemical information is obtained from the number of water molecules lost upon activating large clusters.

1. Introduction

Molecular cluster ions, which have been described as "bridging the gas and condensed phases,"[1] can provide fundamental insight into ion-solvent dynamics, solution-phase phenomena, such as the Hofmeister series,[2] and atmospheric phenomena, such as ion-induced nucleation[3] and aerosol chemistry.[4] Because of the importance of ion-water interactions, extensive effort has gone into investigating the properties of gaseous hydrated ions and how these properties change with cluster size and approach those of bulk solutions. An abundance of information for smaller cluster ions has been reported, including thermodynamic properties (ΔG, ΔH, ΔS, and ΔU) of sequential hydration of numerous elemental cations[5−28] and anions,[28,29] as well as a wide variety of molecular ions.[28,30−33] These and other structural studies, such as spectroscopy,[34−42] resulted in a detailed understanding as to how water organizes around ions, information about ion coordination numbers, and even how water interacts with and affects the structure of biomolecules.[34−36] Extending such measurements to larger cluster sizes is challenging, and experimental results concerning clusters with two or more solvent shells are limited. In principle, it is possible to obtain bulk physical properties by extrapolating data from clusters as a function of size, but this can require measurements obtained from very large clusters. For example, the vertical electron affinity of water has been extrapolated from photoelectron spectroscopy measurements of anionic water clusters with up to 69 water molecules.[43]

The binding energies of water molecules to ionic clusters depend on many factors, including the ion identity, charge state, and cluster size. Effects of ion identity on water binding energies are significant for smaller clusters but rapidly decrease with increasing cluster ion size. For example, values for the binding enthalpy of the first water to $M(H_2O)_n^+$ (M = Li, Na, and K) range from 17.9 to 32.7 kcal/mol,[10,11,19] whereas these values for the sixth water molecule range from 10.0 to 12.1 kcal/mol.[10,11] Similarly, effects of charge on the water binding energy rapidly decrease with cluster size; values for the water binding enthalpy to divalent Mg, Ca, Sr, and Ba are between 11.6 and 13.0 kcal/mol for clusters with 13 water molecules.[20] Few experimental measurements of water binding energies[8,9,44] and enthalpies[8] for significantly larger ionic clusters have been reported.

Accurate thermodynamic values of water binding to large clusters are important for a variety of applications, including modeling ion-induced nucleation[45] and ion nanocalorimetry.[46−49] The latter method recently has been used to provide new insight concerning ion-electron recombination reactions from which information about absolute electrochemical half-cell potentials in bulk solution[48,49] and other bulk physical properties can be obtained. In ion nanocalorimetry, a measure of the internal energy that is deposited into a cluster upon activation is obtained from the distribution of ligands that are lost from the cluster. For example, electron capture by $[Ru(NH_3)_6(H_2O)_{55}]^{3+}$ results in the loss of 17−19 water molecules from the reduced precursor.[48,49] For large clusters such as this, the recombination energy is determined predominantly from the sum of the ligand binding energies for each water molecule lost.[46−49] Because of the large number of water molecules that typically evaporate from the clusters upon ion-electron recombination, accurate values for the binding energy of water as a function of charge

* Corresponding author. Tel.: (510) 643-7161; fax: (510) 642-7714; e-mail: Williams@cchem.berkeley.edu.

10.1021/jp711012b CCC: $40.75
Published on Web 03/22/2008

state and cluster size are essential to obtain accurate bulk properties. Uncertainties concerning the binding energy of each water molecule that evaporates from these reduced clusters add up and contribute significantly to the overall uncertainty of this method.

Because of the paucity of experimental data on large cluster ions and clusters containing multivalent ions with high charge states, an attractive approach is to calculate the thermodynamic properties of water binding using ion-solvation models. Thomson derived an equation to calculate the effect on the vapor pressure of a liquid when confined to a charged spherical drop,[50,51] which increases the vapor pressure versus the bulk. Charging the drop decreases the vapor pressure. This Thomson liquid drop model[50,51] has been used to calculate the thermodynamic properties of ion clustering reactions,[10,52−55] to calculate barriers to nucleation,[52,56] and to correlate single ion-solvation enthalpies with stepwise solvation data.[57] Castleman and Holland calculated sequential binding enthalpies and entropies for monovalent clustering reactions of the form

$$M^+L_n \rightarrow M^+L_{n-1} + L \quad (1)$$

with the Thomson equation using solvent parameters for water, ammonia, pyridine, acetonitrile, and methanol.[53] Values from this continuous charged liquid drop model (C model) were comparable to those obtained from high-pressure mass spectrometry (HPMS) for water, but the agreement for other solvents was not as good. In general, the agreement between the sequential enthalpy calculations and the experimental data was better than that for entropy.

The Thomson liquid drop model and other variants discussed next do not explicitly account for structural effects in the clusters. For small clusters, specific ion-solvent interactions, such as shell structures or magic numbers, can result in deviations from models that are based solely on bulk solvent properties. Such models should provide more accurate thermodynamic values at larger sizes where specific structural effects should be less significant. Because experimental data generally exist for smaller cluster sizes, the effect of cluster structure is an important factor when evaluating such models.

In the Thomson liquid drop model, the charge is located in the center of a homogeneous dielectric sphere. The location of the ion in a cluster depends on the identity of the ion impurity and cluster size. For example, the location of the excess electron (surface vs interior) in hydrated electron clusters and how this depends on cluster size is still hotly debated.[58−61] Hynes and co-workers introduced a surface ion liquid drop model, in which sequential binding thermodynamic values were calculated using the C model but were corrected for a surface-solvated charge.[54] This model also takes into account the volume of the impurity ion, a factor not included in previous models.[52,53,55] To account for the impurity ion volume, absolute solvation free energy data were used to obtain the approximate size exclusion radii for Na^+ and I^- using the Born solvation equation.[62] Hydrated Na^+ and I^- clusters were investigated because Na^+ is solvated internally, whereas I^- is likely to be surface-solvated for n up to ~60.[63,64] Calculated sequential enthalpy and free energy values from the C model and clustering data for $Na(H_2O)_n^+$ at small sizes ($n \leq 6$) were in good agreement, whereas the surface ion liquid drop model performed less well at small cluster sizes when compared to sequential binding enthalpies for $I(H_2O)_n^-$, measured experimentally for $n \leq 5$ and calculated using computer simulations for $n \leq 6$.

A new implementation of the Thomson liquid drop model recently was introduced (referred to in the following text as the DD model), in which clustering reactions are treated discretely, a term for the energy of the permanent dipole and induced dipole interaction between the evaporating ligand and the ionic cluster was introduced, but the model does not include the ion size.[55] The sequential binding enthalpies calculated with this model were compared to sequential solvation enthalpies of protonated water, methanol, ammonia, and pyridine clusters using solvent parameters at various temperatures, including 313 K for water. The calculated values agree relatively well with measured data for protonated clusters. No comparisons to solvated metal ion cluster data were made. The DD model was recently used to develop a second-generation ion-mediated nucleation model.[45]

Because of the strong dependence of these models on charge, comparisons to solvated divalent metal ion data provide a more rigorous test of the validity of such models. Whereas solvated monovalent clusters can be formed readily using association reactions between a metal ion and a solvent vapor, divalent cluster ions can be more difficult to produce because of the possibility of a competitive charge separation pathway at small cluster sizes.[65] Electrospray ionization (ESI)[66] enables the gentle transfer of ions that exist in solution to the gas phase[67] and has been used to produce hydrated divalent[20−26] and even trivalent cluster ions.[68] Thermodynamic values for the sequential binding of water to divalent ions have been measured for numerous ions using HPMS,[20−22,29] black body infrared radiative dissociation (BIRD),[23−25] and guided ion beam mass spectrometry (GIBMS).[26] This body of data presents a prime opportunity to test the various Thomson model implementations for calculating stepwise binding thermodynamic values from strictly macroscopic properties and ascertain the limits of these models.

Here, we compare three variants of the Thomson equation to previously reported experimental mono- and divalent ion clustering thermodynamic data. Effects of charge and temperature on the Thomson equation models were examined, and a slightly modified implementation of the Thomson liquid drop model was found to provide the best fit to experimental data for a wide range of cluster ions of various sizes and charges.

2. Various Implementations of Thomson Model for Calculating Sequential Thermodynamic Properties of Cluster Ions

2.1. Continuous Thomson Model. The free energy to create a cluster ion, ML_n^z, consisting of an ion impurity, M^z, of nominal charge z and solvated by n ligands may be approximated using the Thomson equation,[50,51] in which the energy to condense n ligands is combined with the surface energy required to form the neutral drop (ΔG_{surf}) and the energy to charge the condensed dielectric (or the energy to solvate the charged drop, ΔG_{solv}, using the Born equation).[62] In SI units, the free energy change for drop formation, $\Delta G_{0,n}$, can be expressed by[53]

$$\Delta G_{0,n} = -nkT \ln P_R + 4\pi\gamma R_n^2 + (z^2e^2/8\pi\epsilon_0 R_n)(1 - \epsilon^{-1}) \quad (2)$$

where the first, second, and third terms correspond to the condensation free energy, ΔG_{surf}, and ΔG_{solv}, respectively; k, ϵ_0, and e are the Boltzmann constant, vacuum permittivity, and elementary charge, respectively; T is the temperature; P_R is the ratio of the partial pressure of L to the normal vapor pressure of L at the same temperature; and γ and ϵ are the surface tension and dielectric constant of L, respectively. The radius of the cluster is calculated using

$$R_n = (n + a_i)^{1/3} R_s \quad (3)$$

TABLE 1: Properties of Water at 313[a] and 298 K[b]

T (K)	313.15	298.15
M (g/mol)	18.015	18.015
ρ (g/cm^3)	0.9922	0.9970
$\partial\rho/\partial T$	−0.00038	−0.00026
e	73.15	78.38
$\partial\epsilon/\partial T$	−0.3350	−0.3363
γ (mN/m)	69.56	71.99
$\partial\gamma/\partial T$	−0.1635	−0.1541
ln P^0	−2.6200	−3.464917
$\partial \ln P^0/\partial T$	0.0530	0.0597

[a] From ref 53. [b] Obtained and calculated from ref 69.

where R_s is the effective radius of L, and a_i is a volume factor relating the size of L to the size of the ion impurity. The effective radius is calculated from bulk density data

$$R_s = (3M/4\pi\rho N)^{1/3} \quad (4)$$

where M and ρ are the molar mass and density of L, respectively, and N is Avogadro's constant. The free energy change per addition of a single ligand ($\Delta G_{n,n-1}$) may be approximated by differentiating the negative of eq 2 with respect to size, n,[53] resulting in (SI units)

$$\Delta G_{n,n-1} = -kT \ln P^0 - \gamma(32\pi M^2/3\rho^2 N^2 n)^{1/3} + (z^2e^2/32\pi^2\epsilon_0 N)(1-\epsilon^{-1})(4\pi N/3n)^{4/3} \quad (5)$$

where the first term is the bulk free energy of vaporization (ΔG_{vap}), and P^0 is the vapor pressure of L at temperature T. Stepwise binding entropies ($\Delta S_{n,n-1}$) are calculated by differentiating eq 5 with respect to temperature ($\Delta S = -\partial\Delta G/\partial T$) holding the internal droplet pressure constant. The approximate sequential binding enthalpies ($\Delta H_{n,n-1}$) were obtained from the thermodynamic relationship

$$\Delta H_{n,n-1} = \Delta G_{n,n-1} + T\Delta S_{n,n-1} \quad (6)$$

Results of the C model using physical properties of water at 313 K (Table 1) are shown in Figure 1 for monovalent, divalent, and trivalent ions as a function of cluster size. As expected, higher charge states result in significantly higher calculated $\Delta H_{n,n-1}$ values, and this effect is most pronounced at smaller cluster sizes. For $n = 2$, $\Delta H_{n,n-1}$ equals 18, 54, and 113 kcal/mol for $z = 1$, 2, and 3, respectively. However, for $n = 30$, the difference between $\Delta H_{n,n-1}$ for $z = 1$ and 2 is less than 1 kcal/mol, and for $n = 61$, the difference in $\Delta H_{n,n-1}$ between $z = 1$ and 3 is less than 1 kcal/mol. By $n \approx 350$, the binding enthalpies for the $z = 1-3$ clusters are calculated to be within 0.1 kcal/mol, indicating that the effect of charge state on individual water binding energies is minimal for these larger sizes. The C model for all three charge states converges to the bulk water enthalpy of vaporization (10.3 kcal/mol) as n approaches ∞. For $n = 1000$, the calculated $\Delta H_{n,n-1}$ values of the $z = 1$, 2, and 3 clusters are 9.8 kcal/mol and for $n = 10\,000$, this value is 10.1 kcal/mol. This model predicts that a very large hydration number is needed to reach the corresponding bulk enthalpy value.

2.2. Discrete Thomson Model. With the continuous Thomson model, the discrete phenomenon of sequential ligand evaporation was approximated by a continuous function. Calculating the thermodynamic properties of the product cluster, ML_{n-1}^z, from the slope of this continuous function at the ML_n^z cluster resulted in a systematic deviation that became more significant at smaller cluster sizes (vide infra). The stepwise thermodynamic properties of ligand binding to a metal ion can be discretely calculated using the thermodynamic cycle shown

SCHEME 1

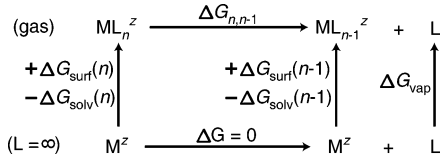

in Scheme 1, where ΔG_{solv}, ΔG_{surf}, and ΔG_{vap} are combined to obtain $\Delta G_{n,n-1}$ of the cluster ML_n^z, resulting

$$\Delta G_{n,n-1} = \Delta G_{solv}(n) - \Delta G_{solv}(n-1) - \Delta G_{surf}(n) + \Delta G_{surf}(n-1) + \Delta G_{vap} \quad (7)$$

Evaluating these equations explicitly for the reactant and product clusters results in

$$\Delta G_{n,n-1} = (z^2e^2/8\pi\epsilon_0)(4\pi\rho N/3M)^{1/3}(1-\epsilon^{-1})[(n+a_i-1)^{-1/3} - (n+a_i)^{-1/3}] + 4\pi\gamma(3M/4\pi\rho N)^{2/3}[(n+a_i-1)^{2/3} - (n+a_i)^{2/3}] - kT\ln P^0 \quad (8)$$

and the entropy was calculated by differentiating the negative of the eq 8 free energy with respect to T at fixed internal droplet pressure, resulting in

$$\Delta S_{n,n-1} = (z^2e^2/8\pi\epsilon_0)(4\pi N/3M)^{1/3}[(n+a_i)^{-1/3} - (n+a_i-1)^{-1/3}][(1/3)(1-\epsilon^{-1})\rho^{-2/3}(\partial\rho/\partial T) + \rho^{1/3}\epsilon^{-2}(\partial\epsilon/\partial T)] - 4\pi(3M/4\pi N)^{2/3}[(n+a_i-1)^{2/3} - (n+a_i)^{2/3}][\rho^{-2/3}(\partial\gamma/\partial T) - (2/3)\gamma\rho^{-5/3}(\partial\rho/\partial T)] + k\ln P^0 + kT(\partial \ln P^0/\partial T) \quad (9)$$

which is combined with eqs 6 and 8 to give the stepwise binding enthalpies.

The results of this discrete Thomson equation (or D model) for the stepwise binding enthalpies for $z = 1$, 2, and 3 are displayed in Figure 1. Comparison to the results of the C model indicates that at larger sizes, the two models are equivalent, but at smaller sizes for which mono- and divalent experimental data exist, binding enthalpies from the C model are lower than those from the D model. This difference is more significant for higher charge states. For $n = 2$, the binding enthalpies from the C model are smaller than those of the D model by ~6, 26, and 60 kcal/mol for $z = 1$, 2, and 3, respectively. The difference between the discrete and the continuous models is less than 0.1 kcal/mol by $n = 9$, 19, and 27 for the monovalent, divalent, and trivalent clusters, respectively. The systematic deviation of the C model as compared to the D model occurs because the slope of the total cluster enthalpy of the n-mer with respect to n at size n is used to extrapolate the enthalpy of the $n - 1$ cluster. The C model enthalpy values are systematically lower because the total cluster enthalpy increases with decreasing cluster size. At small cluster sizes and higher charge states, where the rate of enthalpy change with size is the greatest, the systematic deviation is the most significant.

2.3. Discrete Ion-Dipole Thomson Model. A modified Thomson model was recently introduced that includes the energy required for the evaporating ligand to escape the ion-dipole interaction between the $n - 1$ cluster and the ligand to infinite separation.[55] For this model, the free energy contribution of the interaction between the dipole and cluster ion (ΔG_{IDI}) to the stepwise binding free energy was calculated to be

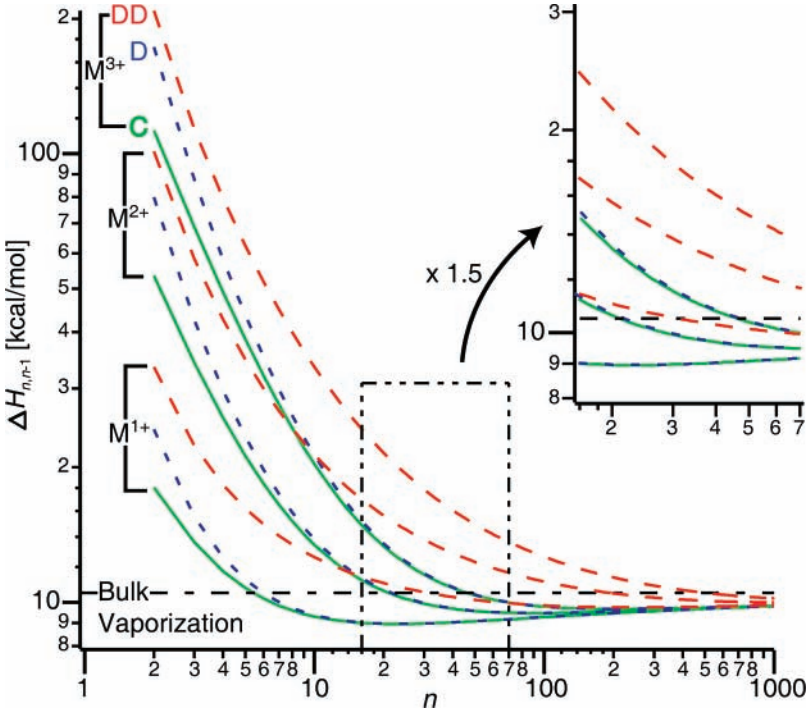

Figure 1. Stepwise binding enthalpies ($\Delta H_{n,n-1}$) calculated as a function of size, n, and nominal charge, z, using the continuous (C), discrete (D), and discrete ion-dipole (DD) Thomson models. Area of interest to recent nanocalorimetry experiments (see ref 49) is scaled by a factor of 1.5.

$$\Delta G_{\mathrm{IDI}} = (1/2)\alpha {E_{n-1}}^2 + kT \ln[\sinh(x)/x] \qquad (10)$$

where $E_{n-1} = ze/(4\pi\epsilon_0(R_n + R_1)^2)$, $x = \mu_0 E_{n-1}/kT$, α is the polarizability of L, and μ_0 is the dipole moment of L. The free energy contribution of the ion-dipole interaction is the force between the ion and both the induced and the permanent dipoles integrated over the reaction coordinate distance for removing L from the surface of ML_n^z to infinite distance. The corresponding entropy (ΔS_{IDI}) was obtained from the differential of the eq 10 free energy with respect to temperature resulting in

$$\Delta S_{\mathrm{IDI}} = -(1/2){E_{n-1}}^2[\partial\alpha/\partial T + (\partial\rho/\partial T)(n-1)M/(\pi N {R_{n-1}}^2(R_{n-1}+R_1)\rho^2)] - k\ln[\sinh(x)/x] + kL(x)x - kTL(x)[{\mu_0}^{-1}(\partial\mu_0/\partial T) + (\partial\rho/\partial T)(n-1)M/(2\pi N {R_{n-1}}^2)(R_{n-1}+R_1)\rho^2] \qquad (11)$$

where $L(x) = [\coth(x)] - x^{-1}$. These terms are combined with eqs 8 and 9 to calculate $\Delta H_{n,n-1}$ values. The temperature dependence of the α and μ_0 terms is not included in the calculated entropy values (i.e., $\partial\alpha/\partial T$ and $\partial\mu_0/\partial T$ are set to zero).

The results of calculating the stepwise binding enthalpies using the DD model are shown in Figure 1. The additional ion-dipole interaction term results in an increase in the calculated binding enthalpy. With both the discrete and the continuous Thomson models, the sequential binding enthalpies reach a local minimum for intermediate n. No such minimum occurs with the DD model (at least for $n \leq 1000$) because the combined magnitude of the ion-dipole term and ion-solvation term exceed that of the surface tension term (vide infra).

2.4. Components to Sequential Clustering Enthalpies and Temperature Effects. The solvation, surface, and bulk heat of vaporization components to the calculated stepwise enthalpy values using the discrete and continuous models are shown in Figure 2. The difference in the solvation enthalpy components between the D and the C models is larger than that for the surface component because the rate of change is larger for the

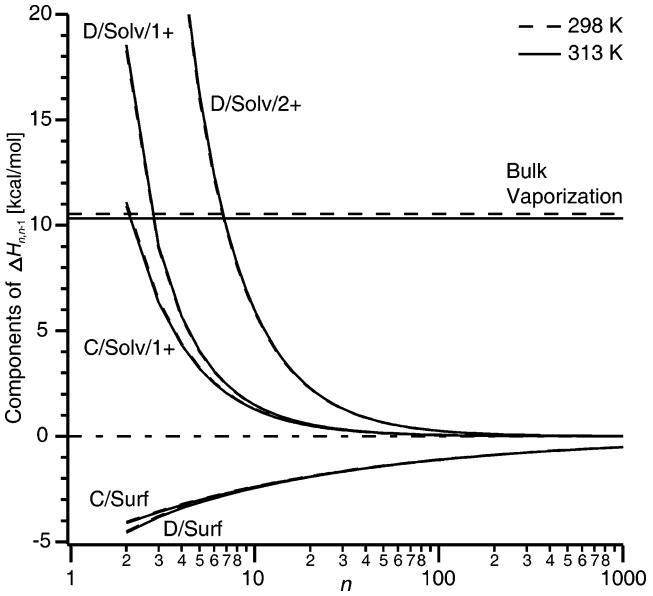

Figure 2. Stepwise enthalpy contributions from the solvation (Solv), surface (Surf), and bulk vaporization terms to $\Delta H_{n,n-1}$ calculated using physical properties of water at 298 and 313 K.

solvation component than the surface component. The solvation enthalpy essentially goes to zero (<0.05 kcal/mol) by $n = 122$ for M^+ and $n = 344$ for M^{2+}, whereas the contribution due to surface enthalpy is -0.5 kcal/mol at $n = 1000$.

It is interesting to examine the effects of temperature upon the various liquid drop model implementations. Castleman and Holland used parameters for bulk water at 313 K,[53] and these same parameters were used in subsequent studies.[54,55] Using the parameters for water at 298 K[69] for all three liquid drop models (see Table 1) resulted in essentially the same values as using 313 K parameters for the surface and solvation enthalpy components, although very subtle differences exist (Figure 2). However, the bulk vaporization enthalpy of water is 10.5 kcal/

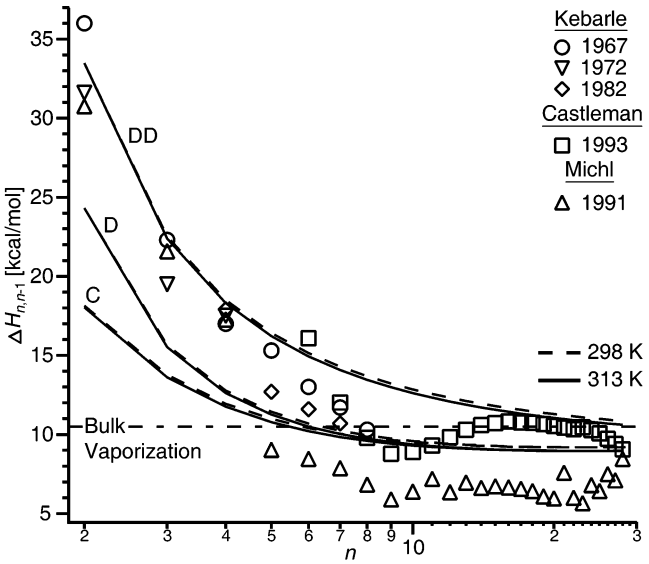

Figure 3. Sequential hydration enthalpy values for monovalent cluster ions calculated using the continuous (C), discrete (D), and discrete ion-dipole (DD) Thomson equations using properties of water at 298 and 313 K. Experimental values for protonated water clusters are from refs 5−9.

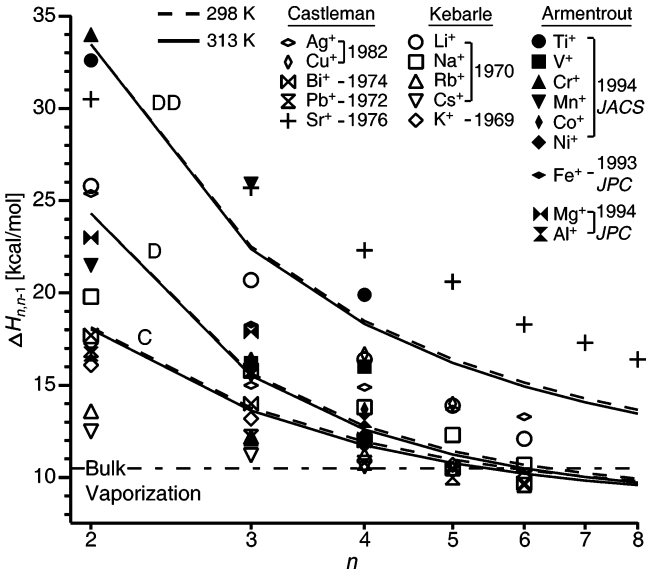

Figure 4. Sequential hydration enthalpy values for monovalent cluster ions calculated using the continuous (C), discrete (D), and discrete ion-dipole (DD) Thomson equations using properties of water at 298 and 313 K. Experimental monovalent metal ion values are from refs 10−18.

mol at 298 K and 10.3 kcal/mol at 313 K. This small difference should not appreciably affect the comparison between experimental and calculated values for small n values but results in a ∼0.2 kcal/mol higher binding enthalpy at larger cluster sizes. This reflects the large contribution from the bulk vaporization value at larger cluster sizes to the calculated $\Delta H_{n,n-1}$ value. This difference is significant for recent nanocalorimetry experiments where energy deposition is determined from the sum of binding enthalpies for a large number of water molecules that are lost.

3. Comparison to Experimental Stepwise Hydration Data

3.1. Monovalent Cluster Ions. A comparison between the C, the D, and the DD models to protonated water sequential hydration data[5−9] is shown in Figure 3. At smaller cluster sizes (n < 9), most of the experimental data are obtained from equilibrium measurements of the stepwise thermodynamic properties of various metal ions using HPMS.[5−7] For n > 8, the sequential hydration energies are obtained exclusively from either metastable ion fractions combined with Klots' model of evaporative dissociation[8] or from collisional induced dissociation experiments.[9] The discrepancy in results obtained from these two methods is significant (∼4 kcal/mol for many values). For n = 6, enthalpy values range from 8.5 to 16.1 kcal/mol.[8,9] Protonated water clusters can form a range of interesting structures[37−39,70,71] that are not accounted for with the various implementations of the Thomson liquid drop model. Both experimental and computational results suggest that $H(H_2O)_{n=5-28}^+$ clusters form chain, single-ring, multiple-rings, or cage-like structures as n increases.[38,71] Spectroscopic results and electronic structure calculations for $H(H_2O)_n^+$, for n = 20,[37,70] 21,[37,39,70] and 28,[39] also suggest that the proton is at the surface of a cage-like structure. At n = 20, sequential enthalpy values calculated using the surface ion liquid drop model[54] are ∼1 kcal/mol lower than that calculated using the C model. Because of the uncertainties in the experimental values and potentially significant structural effects for protonated water clusters, data for other ion clusters in which the charge impurity is located in the interior of the cluster, such as hydrated metal ion data, may provide a more direct comparison to the calculated thermodynamic properties from the Thomson liquid drop models.

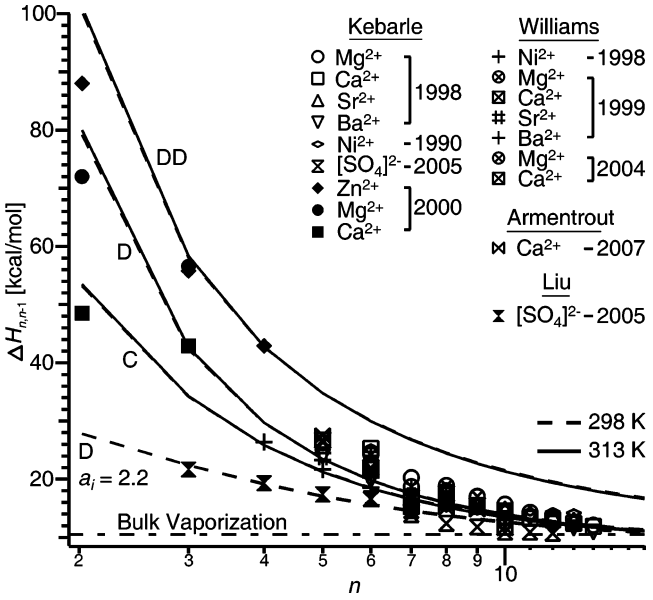

Figure 5. Sequential hydration enthalpy values for divalent cluster ions calculated using the continuous (C), discrete (D) with an ion impurity volume factor (a_i) of 0 and 2.2 corresponding to $[SO_4]^{2-}$, and discrete ion-dipole (DD) Thomson equations using properties of water at 298 and 313 K. Clustering experimental data are from refs 20−26 and 29. Filled symbols are calculated quantum chemical values from ref 73.

A comparison between the C, the D, and the DD models to monovalent hydrated metal ion data[10−15] is shown in Figure 4. The values calculated using the C and D models both agree with most of the experimental data at small sizes better than the DD model, although there is a large variance in the experimental data for different ions, and all three models fit the data relatively well. The DD model is in good agreement with HPMS data for monovalent strontium,[15] but these values appear to be anomalously high. Because the models depend highly on the ionic charge, a more stringent test may be obtained by comparisons to experimental data for divalent ions.

3.2. Divalent Cluster Ions. Stepwise water binding enthalpy values from the C, D, and DD models and experimental data

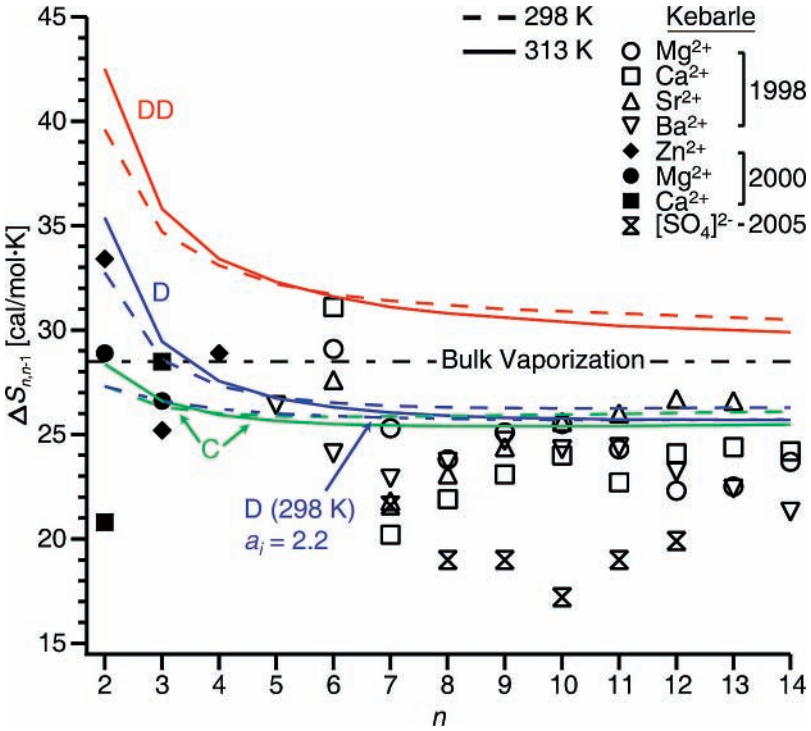

Figure 6. Sequential hydration entropy values for divalent cluster ions calculated using the continuous (C), discrete (D) with an ion impurity volume factor (a_i) of 0 and 2.2 corresponding to $[SO_4]^{2-}$, and discrete ion-dipole (DD) Thomson equations using properties of water at 298 and 313 K. Filled symbols are calculated quantum chemical values from ref 22. Open symbols are experimental data from refs 20 and 29.

for divalent ions measured by HPMS,[20−22] BIRD,[24,25] and GIBMS,[26] as well as select computational values for smaller cluster sizes[22] are compared in Figure 5. Values obtained using the DD model are higher than the largest measured binding enthalpy data by ∼2 to ∼4 kcal/mol for $n = 6-14$, and in this size range, both the C and the D models clearly perform better. Thermodynamic values obtained from the Thomson model depend only on the initial and final states of the evaporation process. The ion-dipole term in the DD model adds some of the reaction path energy to the thermochemical values based on the initial and final states and in doing so erroneously accounts for the ion-molecule interactions. The anomalously high values for the DD model are directly attributable to this additional ion-dipole term that essentially takes into account electrostatic interactions between the ion and the molecule twice. At the smallest sizes, where the Thomson models are expected to perform the worst, all models fit the calculated data moderately well.

As for the monovalent clusters, the binding enthalpies for the divalent clusters depend strongly on ion identity at small sizes, but these values converge for larger n. At $n = 6$ and 12, the divalent experimental sequential enthalpy values span a range of ∼7 and ∼4 kcal/mol, respectively. The average absolute difference between the D model and the experimental data is 2.9 and 0.9 kcal/mol at $n = 6$ and 12, respectively. At $n = 6$ and 12, the average absolute difference between the C model and the experiment is 4.0 and 1.0 kcal/mol, respectively.

To evaluate the effect of ion volume on the D model, $\Delta H_{n,n-1}$ values that include the calculated size exclusion volume for $[SO_4]^{2-}$, $a_i = 2.2$, are shown (lower curve in Figure 5). The a_i value is obtained from the absolute solvation energy (−260.5 kcal/mol)[72] of $[SO_4]^{2-}$ and the Born equation.[62] The size exclusion volume of $[SO_4]^{2-}$ is larger than that of the other impurity ions (especially those that are positively charged) and thus represents an upper limit to this effect for the ions investigated (the other limit corresponding to $a_i = 0$). Including the size exclusion volume of the impurity ion with the D model results in a lower binding enthalpy, and the agreement with both calculated quantum chemical values[73] and experimental values[29] for $[SO_4(H_2O)_n]^{2-}$ is excellent. However, the range in experimental values for clusters of a given size that contains different impurity ions is greater. This may be due to specific structural effects, although uncertainties in the experimental measurements also may contribute significantly to the range in values. At larger sizes, the ion volume does not significantly affect the calculated binding enthalpies. At $n = 24$, the difference in binding enthalpies for $a_i = 0$ and 2.2 is less than ∼0.1 kcal/mol.

Because the Thomson models are based on bulk physical properties of the solvent, specific structural effects are not taken into account. It is interesting to compare entropy data because structural differences can cause relatively large changes in entropy. Sequential binding entropy data have been compared to calculated values for monovalent cluster ions.[52,53,55] Yu showed that the sequential binding entropies calculated by the DD model agree better than the C model for protonated water, methanol, ammonia, and acetonitrile clusters.[55] However, for small water clusters, both models agree reasonably well. To better test the limits of the Thomson models, calculated entropy values are compared to experimental data for hydrated divalent ions in Figure 6. Values from the DD model are much higher than the experimental values. Both the continuous and the discrete models (for both $a_i = 0$ and 2.2) provide better agreement.

Although the Thomson drop model does not take into account specific ion effects, the model does remarkably well at accounting for charge effects at small cluster sizes. Specific ion effects and solvent orientation might be expected to be more significant for divalent than monovalent ions, yet both the C and the D models appear to fit the data for these two different charged clusters equally well. Thus, although an ion may lower the effective dielectric constant of the solvent near the ion[74] and the presence of a charge in a drop may alter the surface tension,[75]

these effects should increase with charge state. The generally good agreement between the Thomson drop model and the experimental data for mono- and divalent ions suggests that these effects may not be very large.

4. Conclusion

The Thomson equation is a robust macroscopic model from which thermodynamic data for the evaporation of solvent from clusters can be obtained. The performance of various implementations of this model was compared for hydrated clusters containing both mono- and divalent ions. For hydrated clusters containing monovalent ions, all the models appear to fit existing experimental data reasonably well given the expected limitations of these models. However, for hydrated divalent ions, the continuous model[53] and a discrete model that takes into account effects of the excluded volume of the impurity ion perform significantly better than a recently proposed model that includes an ion-dipole term.[55] For smaller clusters, the systematic deviation introduced by the continuous model results in significantly lower binding enthalpies than those calculated from the discrete model, but this difference becomes negligible for larger clusters.

In earlier work, physical properties of water at a temperature of 313 K were used. For small clusters, effects of temperature are negligible, and parameters of water at 298 K resulted in nearly the same water binding enthalpies and entropies. However, effects of temperature are more significant at larger cluster sizes for which there is limited or no experimental data. With parameters for water at 298 K, binding enthalpies are ~0.2 kcal/mol higher for $n \geq 4$ and 10 for $z = 1$ and 2, respectively. Although small, this effect is significant for the ability to accurately obtain thermodynamic properties from recent ion nanocalorimetry experiments in which energy deposition is obtained primarily from the sum of binding enthalpies for each water molecule that evaporates from a cluster.[46−49] When energy deposition is large, a small uncertainty in binding energy values results in a large uncertainty in the sum of these values because the number of water molecules that are lost can be quite large.[48,49] In establishing a value for the absolute standard hydrogen electrode potential versus a free electron using this nanocalorimetry method with clusters containing 55 water molecules,[49] a 0.2 kcal/mol difference in binding enthalpy values resulted in a 0.2 V difference in the value of the SHE. Improved models for obtaining thermochemical data of large ionic clusters can greatly enhance the accuracy with which such nanocalorimetry experiments can be applied. Comparisons of various models to data for multivalent ions of even higher charge states as well as those that are solvated by ligands other than water also should provide an important test of these models.

Acknowledgment. The authors thank James S. Prell for helpful discussions and the NSF (CHE-0718790) and NIH (R01 GM064712-07) for generous financial support.

References and Notes

(1) Castleman, A. W., Jr.; Keesee, R. G. *Acc. Chem. Res.* **1986**, *19*, 413−419.
(2) Kunz, W.; Lo Nostro, P.; Ninham, B. W. *Curr. Opin. Colloid Interface Sci.* **2004**, *9*, 1−18.
(3) Mason, B. J. *The Physics of Clouds*, 2nd ed.; Clarendon Press: Oxford, 1971; pp 1−30.
(4) Reid, J. P.; Sayer, R. M. *Chem. Soc. Rev.* **2003**, *32*, 70−79.
(5) Kebarle, P.; Searles, S. K.; Zolla, A.; Scarborough, J.; Arshadi, M. *J. Am. Chem. Soc.* **1967**, *89*, 6393−6399.
(6) Cunningham, A. J.; Payzant, J. D.; Kebarle, P. *J. Am. Chem. Soc.* **1972**, *94*, 7627−7632.
(7) Lau, Y. K.; Ikuta, S.; Kebarle, P. *J. Am. Chem. Soc.* **1982**, *104*, 1462−1469.
(8) Shi, Z.; Ford, J. V.; Wei, S.; Castleman, A. W., Jr. *J. Chem. Phys.* **1993**, *99*, 8009−8015.
(9) Magnera, T. F.; David, D. E.; Michl, J. *Chem. Phys. Lett.* **1991**, *182*, 363−369.
(10) Džidič, I.; Kebarle, P. *J. Phys. Chem.* **1970**, *74*, 1466−1474.
(11) Searles, S. K.; Kebarle, P. *Can. J. Chem.* **1969**, *47*, 2619−2627.
(12) Holland, P. M.; Castleman, A. W., Jr. *J. Chem. Phys.* **1982**, *76*, 4195−4205.
(13) Tang, I. N.; Castleman, A. W., Jr. *J. Chem. Phys.* **1974**, *60*, 3981−3986.
(14) Tang, I. N.; Castleman, A. W., Jr. *J. Chem. Phys.* **1972**, *57*, 3638−3644.
(15) Tang, I. N.; Lian, M. S.; Castleman, A. W., Jr. *J. Chem. Phys.* **1976**, *65*, 4022−4027.
(16) Schultz, R. H.; Armentrout, P. B. *J. Phys. Chem.* **1993**, *97*, 596−603.
(17) Dalleska, N. F.; Tjelta, B. L.; Armentrout, P. B. *J. Phys. Chem.* **1994**, *98*, 4191−4195.
(18) Dalleska, N. F.; Honma, K.; Sunderlin, L. S.; Armentrout, P. B. *J. Am. Chem. Soc.* **1994**, *116*, 3519−3528.
(19) Rodgers, M. T.; Armentrout, P. B. *J. Phys. Chem.* **1997**, *101*, 1238−1249.
(20) Peschke, M.; Blades, A. T.; Kebarle, P. *J. Phys. Chem. A* **1998**, *102*, 9978−9985.
(21) Blades, A. T.; Jayaweera, P.; Ikonomou, M. G.; Kebarle, P. *Int. J. Mass Spectrom. Ion Processes* **1990**, *102*, 251−267.
(22) Peschke, M.; Blades, A. T.; Kebarle, P. *J. Am. Chem. Soc.* **2000**, *122*, 10440−10449.
(23) Rodriguez-Cruz, S. E.; Jockusch, R. A.; Williams, E. R. *J. Am. Chem. Soc.* **1998**, *120*, 5842−5843.
(24) Rodriguez-Cruz, S. E.; Jockusch, R. A.; Williams, E. R. *J. Am. Chem. Soc.* **1999**, *121*, 8898−8906.
(25) Wong, R. L.; Paech, K.; Williams, E. R. *Int. J. Mass Spectrom.* **2004**, *232*, 59−66.
(26) Carl, D. R.; Moision, R. M.; Armentrout, P. B. *Int. J. Mass Spectrom.* **2007**, *265*, 308−325.
(27) Dalleska, N. F.; Honma, K.; Armentrout, P. B. *J. Am. Chem. Soc.* **1993**, *115*, 12125−12131.
(28) Keesee, R. G.; Castleman, A. W., Jr. *J. Phys. Chem. Ref. Data* **1986**, *15*, 1011−1071.
(29) Blades, A. T.; Kebarle, P. *J. Phys. Chem. A* **2005**, *109*, 8293−8298.
(30) Lemoff, A. S.; Bush, M. F.; Williams, E. R. *J. Am. Chem. Soc.* **2003**, *125*, 13576−13584.
(31) Wyttenbach, T.; Liu, D.; Bowers, M. T. *Int. J. Mass Spectrom.* **2005**, *240*, 221−232.
(32) Kohtani, M.; Breaux, G. A.; Jarrold, M. F. *J. Am. Chem. Soc.* **2004**, *126*, 1206−1213.
(33) Lemoff, A. S.; Williams, E. R. *J. Am. Soc. Mass Spectrom.* **2004**, *15*, 1014−1024.
(34) Bush, M. F.; Prell, J. S.; Saykally, R. J.; Williams, E. R. *J. Am. Chem. Soc.* **2007**, *129*, 13544−13553.
(35) Kamariotis, A.; Boyarkin, O. V.; Mercier, S. R.; Beck, R. D.; Bush, M. F.; Williams, E. R.; Rizzo, T. R. *J. Am. Chem. Soc.* **2006**, *128*, 905−916.
(36) Blom, M. N.; Compagnon, I.; Polfer, N. C.; von Helden, G.; Meijer, G.; Suhai, S.; Paizs, B.; Oomens, J. *J. Phys. Chem. A* **2007**, *111*, 7309−7316.
(37) Shin, J.-W.; Hammer, N. I.; Diken, E. G.; Johnson, M. A.; Walters, R. S.; Jaeger, T. D.; Duncan, M. A.; Christie, R. A.; Jordan, K. D. *Science* **2004**, *304*, 1137−1140.
(38) Miyazaki, M.; Fujii, A.; Ebata, T.; Mikami, N. *Science* **2004**, *304*, 1134−1137.
(39) Wu, C.-C.; Lin, C.-K.; Chang, H.-C.; Jiang, J.-C.; Kuo, J.-L.; Klein, M. L. *J. Chem. Phys.* **2005**, *122*, 74315.
(40) Bush, M. F.; Saykally, R. J.; Williams, E. R. *ChemPhysChem* **2007**, *8*, 2245−2253.
(41) Walters, R. S.; Pillai, E. D.; Duncan, M. A. *J. Am. Chem. Soc.* **2005**, *127*, 16599−16610.
(42) Miller, D. J.; Lisy, J. M. *J. Chem. Phys.* **2006**, *124*, 24319.
(43) Coe, J. V.; Lee, G. H.; Eaton, J. G.; Arnold, S. T.; Sarkas, H. W.; Bowen, K. H.; Ludewigt, C.; Haberland, H.; Worsnop, D. R. *J. Chem. Phys.* **1990**, *92*, 3980−3982.
(44) Arnold, S. T.; Morris, R. A.; Viggiano, A. A.; Johnson, M. A. *J. Phys. Chem.* **1996**, *100*, 2900−2906.
(45) Yu, F. *Atmos. Chem. Phys.* **2006**, *6*, 5193−5211.
(46) Leib, R. D.; Donald, W. A.; Bush, M. F.; O'Brien, J. T.; Williams, E. R. *J. Am. Chem. Soc.* **2007**, *129*, 4894−4895.
(47) Leib, R. D.; Donald, W. A.; Bush, M. F.; O'Brien, J. T.; Williams, E. R. *J. Am. Soc. Mass Spectrom.* **2007**, *18*, 1217−1231.

(48) Leib, R. D.; Donald, W. A.; O'Brien, J. T.; Bush, M. F.; Williams, E. R. *J. Am. Chem. Soc.* **2007**, *129*, 7716−7717.
(49) Donald, W. A.; Leib, R. D.; O'Brien, J. T.; Bush, M. F.; Williams, E. R. *J. Am. Chem. Soc.* **2008**, *130*, 3371−3381.
(50) Thomson, J. J. *Applications of Dynamics and Chemistry*; Macmillan and Co.: London, 1888; pp 165−166.
(51) Thomson, J. J. *Conduction of Electricity through Gases*; C. J. Clay and Sons: London, 1903; pp 149−150.
(52) Castleman, A. W., Jr.; Holland, P. M.; Keesee, R. G. *J. Chem. Phys.* **1978**, *68*, 1760−1767.
(53) Holland, P. M.; Castleman, A. W., Jr. *J. Phys. Chem.* **1982**, *86*, 4181−4188.
(54) Peslherbe, G. H.; Ladanyi, B. M.; Hynes, J. T. *J. Phys. Chem. A* **1999**, *103*, 2561−2571.
(55) Yu, F. *J. Chem. Phys.* **2005**, *122*, 84503.
(56) Castleman, A. W., Jr.; Tang, I. N. *J. Chem. Phys.* **1972**, *57*, 3629−3638.
(57) Lee, N.; Keesee, R. G.; Castleman, A. W., Jr. *J. Colloid Interface Sci.* **1980**, *75*, 555−565.
(58) Turi, L.; Sheu, W. S.; Rossky, P. J. *Science* **2005**, *309*, 914−917.
(59) Verlet, J. R. R.; Bragg, A. E.; Kammrath, A.; Cheshnovsky, O.; Neumark, D. M. *Science* **2005**, *307*, 93−96.
(60) Verlet, J. R. R.; Bragg, A. E.; Kammrath, A.; Cheshnovsky, O.; Neumark, D. M. *Science* **2005**, *310*, 1769.
(61) Barnett, R. N.; Landman, U.; Cleveland, C. L.; Jortner, J. *Phys. Rev. Lett.* **1987**, *59*, 811−814.
(62) Born, M. *Z. Physik* **1920**, *1*, 45−48.
(63) Coe, J. V. *J. Phys. Chem. A* **1997**, *101*, 2055−2063.
(64) Koch, D. M.; Peslherbe, G. H. *Chem. Phys. Lett.* **2002**, *359*, 381−389.
(65) Beyer, M.; Williams, E. R.; Bondybey, V. E. *J. Am. Chem. Soc.* **1999**, *121*, 1565−1573.
(66) Yamashita, M.; Fenn, J. B. *J. Phys. Chem.* **1984**, *88*, 4451−4459.
(67) Fenn, J. B.; Mann, M.; Meng, C. K.; Wong, S. F.; Whitehouse, C. M. *Mass Spectrom. Rev.* **1990**, *9*, 37−70.
(68) Bush, M. F.; Saykally, R. J.; Williams, E. R. *Int. J. Mass Spectrom.* **2006**, *253*, 256−262.
(69) Lide, D. R. *CRC Handbook of Chemistry and Physics, Internet Version*, 87th ed.; Taylor and Francis: Boca Raton, FL, 2007.
(70) Singh, N. J.; Park, M.; Min, S. K.; Suh, S. B.; Kim, K. S. *Angew. Chem., Int. Ed.* **2006**, *45*, 3795−3800.
(71) Chang, H.-C.; Wu, C.-C.; Kuo, J.-L. *Int. Rev. Phys. Chem.* **2005**, *24*, 553−578.
(72) Marcus, Y. *Ion Solvation*; Wiley Interscience: Chichester, U.K., 1985; p 109.
(73) Gao, B.; Liu, Z.-F. *J. Chem. Phys.* **2005**, *123*, 224302.
(74) Booth, F. *J. Chem. Phys.* **1951**, *19*, 391−394.
(75) Buff, F. P.; Stillinger, F. H., Jr. *J. Chem. Phys.* **1956**, *25*, 312−318.